Biochemical Pharmacology 79 (2010) 1516–1525

Contents lists available at ScienceDirect

Biochemical Pharmacology

journal homepage: www.elsevier.com/locate/biochempharm

Identification of metabolic pattern and bioactive form of resveratrol in human medulloblastoma cells

Xiao-Hong Shu, Hong Li, Zheng Sun, Mo-Li Wu, Jing-Xin Ma, Jian-Min Wang, Qian Wang, Yuan Sun, Yuan-Shan Fu, Xiao-Yan Chen, Qing-You Kong, Jia Liu *

Liaoning Laboratory of Cancer Genomics and Department of Cell Biology, College of Basic Medical Sciences, Dalian Medical University, Dalian 116044, China

ARTICLE INFO

Article history:
Received 14 December 2009
Received in revised form 18 January 2010
Accepted 19 January 2010

Keywords:
Resveratrol
Medulloblastoma
Drug metabolism
Sulfotransferase
Chemosensitivity

ABSTRACT

Cancer preventive reagent *trans*-resveratrol is intracellularly biotransformed to different metabolites. However, it is still unclear whether *trans*-resveratrol exerts its biological effects directly or through its metabolite(s). This issue was addressed here by identifying the metabolic pattern and the bioactive form of resveratrol in a resveratrol-sensitive human medulloblastoma cell line, UW228-3. The cell lysates and condition media of UW228-3 cells with or without 100 μM resveratrol treatment were analyzed by HPLC and LC/MS which revealed (1) that resveratrol was chemically unstable and the spontaneous generation of *cis*-resveratrol reduced resveratrol's anti-medulloblastoma efficacy and (2) that resveratrol monosulfate was the major metabolite of the cells. To identify the bioactive form of resveratrol, a mixture-containing approximately half fraction of resveratrol monosulfate was prepared by incubating *trans*-resveratrol with freshly prepared rat brain lysates. Medulloblastoma cells treated by 100 μM of this mixture showed attenuated cell crisis. The overall levels of the three brain-associated sulfotransferases (SULT1A1, 1C2 and 4A1) were low in medulloblastoma cells in vivo and in vitro in comparison with that in human noncancerous and rat normal cerebella; resveratrol could more or less up-regulate the production of these enzymes in UW228-3 cells but their overall level was still lower than that in normal cerebellum tissue. Our study thus demonstrated for the first time that *trans*-resveratrol is the bioactive form in medulloblastoma cells in which the expression of brain-associated SULTs was down-regulated, resulting in the increased intracellular bioavailability and anti-medulloblastoma efficacy of *trans*-resveratrol.

1. Introduction

Resveratrol (3,5,4′-trihydroxy-*trans*-stilbene, Res) is a plant polyphenol existing in grapes and many other natural foods [1,2], which possesses a wide range of biological activities such as cardiovascular protection [3,4], antioxidative activity [5], anti-inflammatory property [6,7], and cancer preventive and therapeutic effects [8,9]. It was found that resveratrol affected carcinogenic process by inhibiting cancer-associated gene expression [10,11], altering multiple signaling pathways and/or modulating epigenetic machineries [12,13]. More importantly, this compound has little cytotoxic effect and is able to penetrate blood–brain barrier [14], suggesting its potential therapeutic values in the management of brain malignancies especially those occur at childhood.

It has been recognized that resveratrol, as a polyphenol compound, can be biotransformed intracellularly by multiple metabolic enzymes. Although the chemotherapeutic value and molecular effects of resveratrol have been demonstrated in many types of cancers [11,15–19], it is still unclear whether *trans*-resveratrol exerts its anticancer effects directly or through its metabolite(s) [20]. So far, no direct evidence has been available concerning the anticancer activity of the parent and conjugated resveratrol because of the difficulty to maintain resveratrol unmetabolized in vivo and to fully transform resveratrol to an identical conjugate in vitro. As an alternative approach, it would be worthwhile to elucidate the molecular bases and potential

Abbreviations: Resveratrol, Res or R; HPLC, high performance liquid chromatography; MS, mass spectrum; LC/MS, liquid chromatography coupled with tandem mass spectrum; SULT, sulfotransferases; MB, medulloblastoma; DMEM, Dulbecco's modified Eagle's essential medium; ICC, immunocytochemical staining; TUNEL, terminal deoxynucleotidyl transferase mediated nick end labeling; PBS, phosphate buffered saline solution; SPE, solid phase extraction; ESI, electrospray ionisation; FWHM, full width at half maximum; TMA, the tissue microarray; IHC, immunohistochemical staining; DAB, 3,3′-diaminobenzidine tetrahydrochloride; SDS-PAGE, sodium dodecylsulfate polyacrylamide gel electrophoresis; N2, nebulizing gas; LC/MS-IT-TOF, ion trap-time-of-flight hybrid mass spectrometer; HRMS, high resolution mass spectrometry; Mops, 3-[N-morpholino] propanesulfonic acid; PAPS, 3′-phosphoadenosine 5′-phosphosulfate; DTT, dithiothreitol; STAT3, signal transducer and activator of transcription 3; RT-PCR, reverse transcription-polymerase chain reaction; TIC, total ion chromatogram; CID, collision induced dissociation.

* Corresponding author. Tel.: +86 411 86110316; fax: +86 411 86110278.
E-mail address: jialiudl@yahoo.com.cn (J. Liu).

0006-2952/$ – see front matter © 2010 Elsevier Inc. All rights reserved.
doi:10.1016/j.bcp.2010.01.022

therapeutic implications of resveratrol metabolism using a reliable resveratrol-sensitive cancer cells.

Medulloblastoma (MB) is originated from primitive neural precursor cells in the external germinal layer of the developing cerebellum and accounts for more than 25% of cancer-related death among child patients [21]. Great majority of MB patients has poor prognosis and suffers from direct surgical damages, long-term side effects and developmental defects [22]. Therefore, a more effective and less toxic therapeutic approach is urgently required for better treatment of MBs. It has been recognized that MBs maintain the potential for further differentiation when exposed to differentiation promoters [23]. According to our results obtained from four human MB cell lines [11,15,16,24], resveratrol possessed anti-medulloblastoma capacity through promoting both neuronal-like differentiation and apoptosis by arresting cell cycle at G1 phase and down-regulating a panel of cancer-associated gene expression in MB cells presumably through altering the activities of several signaling pathways. The resveratrol-sensitive feature of MB cells thus offers us an ideal model to shed light on the metabolic pattern and the bioactive form of resveratrol in cancer cells.

2. Materials and methods

2.1. Cell culture and treatments

Human medulloblastoma cell line UW228-3 [25] were cultured in Dulbecco's modified Eagles medium (DMEM; Invitrogen Co., Grand Island, NY, USA) containing 10% fetal bovine serum (Invitrogen Co., Grand Island, NY, USA) under 37 °C and 5% CO_2 condition. The cells (5×10^4/mL) were plated to 100 mm dishes (Nunc A/S, Roskilde, Denmark) and incubated for 24 h before further experiments. For morphologic evaluation and ICC staining, the coverslips were put into the dishes before initial cell seeding and collected in 6 h intervals during the experiments.

Stock solution of 100 mM *trans*-resveratrol (Sigma Chem Co., St. Louis, MO, USA) was prepared in dimethylsulfoxide (DMSO; Sigma Chem Co., St. Louis, MO, USA), wrapped in aluminium foil for protection against light and stored at −20 °C. *cis*-Resveratrol was prepared by exposure of *trans*-resveratrol-containing solution to natural light for 48 h [26]. Resveratrol were diluted with culture medium to an optimal working concentration (100 μM; 11) just before cell treatment. The cells incubated with the same concentration of DMSO (0.2%) were used as background control. After being treated by 100 μM resveratrol for 48 h, the cells as well as their culture media were collected respectively and analyzed by HPLC and LC/MS. The remaining cells were used for paralleled protein and RNA preparations and flow cytometry analysis. The total numbers and the viability of cells with or without 100 μM resveratrol treatment were determined by staining the single-cell suspensions with 0.25% Trypan Blue (Sigma Chem Co., St. Louis, MO, USA) and counting the stained and unstained cells with the hemocytometers by two independent researchers. Cell-bearing coverslips were harvested at 48 h time point and fixed properly for morphologic examination, immunocytochemical (ICC) staining and terminal deoxynucleotidyl transferase mediated nick end labeling (TUNEL; Promega Corp., Madison, WI, USA) by the methods described elsewhere [16]. Each of experimental groups was set in triplicate, and the experiments were repeated at least three times to establish confidential conclusions. The antibodies used for ICC staining were the mouse anti-human synaptophysin antibody (Santa Cruz Inc., CA, USA: 1:120) and the rabbit anti-human SULT1A1, 1C2 and 4A1 antibodies (1:120, 1:100 and 1:120; Protein Tech Group, Inc., Chicago, USA).

2.2. Sample preparation for HPLC and LC/MS analyses

After resveratrol treatment, the cells were scraped off, washed three times with PBS (pH 7.4), and lysed by sonication. Meanwhile, cell-free media were harvested directly by the end of 48-h resveratrol treatment or after an additional 24-h normal culture. The collected media and cell lysates were centrifuged at 10,000 × *g* for 5 min, and the supernatants were purified by SPE [27]. Briefly, Cleanert PEP-SPE cartridges (60 mg; Agela Technol Inc. PA, USA) were conditioned with 5 mL of methanol (Fisher Sci, Fair Lawn, NJ, USA) and then with 5 mL of ultrapure water purified with a Milli-Q water purification system (Millipore, Bedford, MA, USA). The samples were loaded onto the cartridges, and the cartridges were washed with 5 mL of ultrapure water after absorption of the samples on the solid phase. The samples were finally eluted with 3 mL of methanol, and the eluate was dried by nitrogen spraying. The residues were dissolved in 500 μL methanol and a 10 μL aliquot was injected onto the liquid chromatography column for HPLC and LC/MS analysis.

2.3. HPLC analysis

Four kinds of samples were prepared from UW228-3 cell lines as Sample 1, the culture medium treated with 100 μM resveratrol for 48 h; Sample 2, 24-h culture medium after 100 μM resveratrol treatment for 48 h; Sample 3, the cells treated with 100 μM resveratrol for 48 h; Sample 4, resveratrol-containing medium as background control.

The HPLC system (Waters Co., Milford, MA, USA) is consisted of a Waters 1525 binary pump and 2487 dual wavelength UV–vis detector. The detection was carried out at 306 nm [28]. Chromatographic separation of resveratrol and its metabolite(s) was performed on a Hypersil BDS-C18 column (5 μm, 4.6 mm × 250 mm, Elite, Dalian, China), preceded by a C18 guard column (5 μm, 4.6 mm × 10 mm), using a column oven set at 35 °C with a flow rate of 1 mL/min. The mobile phase consisted of 5 mM ammonium acetate (mobile phase A, Alfa Aesar, A Johnson Matthey Company, Ward Hill, MA, USA), and methanol (mobile phase B). These solutions were degassed by sonication for 15 min at room temperature prior to use. A gradient elution was carried out as follows [29]: 0 min, 10% B; 4 min, 20% B; 7 min, 80% B; 16 min, 55% B; 18 min, 55% B; 19 min, 90% B; 25 min, 90% B. Subsequently, the percentage of methanol was decreased within 5 min to 10% in order to equilibrate the column for 10 min before application of the next injection. Samples were filtered through a 0.45 μm filter (Millipore, Bedford, MA, USA) and a 10 μL aliquot was injected.

2.4. Structural identification of resveratrol metabolite(s)

Chromatography was performed on a Agilent 1200 liquid chromatography series (Agilent Technol Inc., Santa Clara, CA, USA) coupled to an Applied Biosystems API 3200 QTrap tandem mass spectrometer (Applied Biosystem/MDS SCIEX, Foster City, CA, USA) equipped with an ESI source, and operated by Applied Biosystem/MDS SCIEX analyst software (Version 1.4.1) to obtain the MS and MS/MS data. The separation was carried out using a C18 reverse phase Hypersil BDS-C18 column (5 μm, 4.6 mm × 250 mm, Elite, Dalian, China) with a guard column. 5 mM ammonium acetate was used as solvent A, and methanol as solvent B, at a flow rate of 0.5 mL/min with the following gradient: 10–20% B linear (0–4 min), 20–80% B linear (4–7 min), 80–55% B linear (7–16 min), 55–90% B (18–19 min), 90–10% B (25–30 min). This was followed by a 10-min equilibrium period with initial conditions prior to injection of the next sample. After being filtered in the filter (0.45 μM, Millipore), 10 μL of the sample was directly injected into the column.

Table 1
Primer sequences used for RT-PCR.

Parameters	Primer sequence (5′ → 3′)	Annealing temperature	Product (bp)
SULT1A1	Forward 5′-GCAACGCAAAGGATGTGGCA-3′ Reverse 5′-TCCGTAGGACACTTCTCCGA-3′	60 °C	122
SULT1C2	Forward 5′-GGTTTGGGGTTCCTGGTTTGAC-3′ Reverse 5′-GGCTGGGACTGAAGGATTGAAG-3′	58 °C	460
SULT4A1	Forward 5′-AGATTCCTGGGGGTGTCCT-3′ Reverse 5′-GTGAGCATGCAGGTTGTTGT-3′	58 °C	250
β-Actin	Forward 5′-GCATGGAGTCCTGTGGCAT-3′ Reverse 5′-CATGAAGCATTTGCGGTGG-3′	58 °C	326

The MS analysis was performed in a negative ion mode. Prior to use, the ion spray interface and mass spectrometric parameters were optimized to obtain maximum sensitivity at unit resolution. The source temperature was set at 250 °C with a curtain gas pressure (N_2) of 25 psi, a N_2 pressure of 30 psi, an auxiliary heat gas pressure of 40 psi. The ion sprayer voltage was set at 5000 V for negative ion mode with a declustering potential of 45 V. The collision energy was set at 10 V and collision gas (N_2) was set at high. Full-scan data acquisition was performed by scanning from m/z 100 to 600 in profile mode [30], using a cycle time of 2 s and a pause between scans of 2 ms. For MS/MS, a product ion scan was used at a cycle time of 2 s. To identify the characteristic ions for each compound, samples were injected into the LC/MS-system in negative ionisation mode.

Further identification and confirmation of the metabolites was performed on a Shimadzu LCMS-IT-TOF (Shimadzu Co., Kyoto, Japan) instrument equipped with an ESI source in negative ion mode at a resolution of 10,000 FWHM. Accurate masses were corrected by using the standard sample sodium trifluoroacetate. 10 μL sample was injected onto a Shim-pack VP-ODS column (5 μm, 2.0 mm × 150 mm; Shimadzu Co., Kyoto, Japan), then was eluted (0.2 mL/min) with a gradient of 5–65% acetonitrile (Alfa Aesar, A Johnson Matthey Company, Ward Hill, MA, USA) in 5 mM ammonium, over 25 min with column temperature maintained at 40 °C. To avoid the cross contamination, the blank run was inserted between the consecutive samples. HRMS analytical conditions were as follows: acquisition m/z, 100–800; interface voltage, 4.50 kV; IT area vacuum, 1.2×10^{-2} Pa; TOF area vacuum, 1.2×10^{-4} Pa; equipment temperature, 40 °C; N_2 flow, 1.5 L/min; drying gas (N_2) pressure, 0.2 MPa; CDL and heater block temperature, 200 °C; interface voltage, 4.50 kV; ion accumulation, 20 ms. MS data were processed with LC/MS solution ver. 3.4 software (Shimadzu, Japan).

2.5. Immunohistochemical staining for sulfotransferases (SULTs)

Surgical specimens were incised from 37 medulloblastoma cases in the range from 9- to 23-year-old. After getting the consents from the patients and/or their parents, the fresh specimens of the tumor mass and, where possible, tumor-surrounding tissues were collected from the operation rooms of the First Affiliated Hospital, Dalian Medical University and Sheng-Jing Hospital, China Medical University at Shenyang within 2 h, fixed in 10% formaldehyde and treated conventionally for preparing paraffin-embedded tissue blocks. The tissue microarrays (TMAs) in a density of 42 tissue spots/cm^2 was constructed using the target tissues cored from the tumors, the surrounding cerebellum regions and rat normal cerebella. Three members of SULT1A1, SULT1C2 and SULT4A1 were selected for TMA-based immunohistochemical staining (IHC) because of their preferential expression in cerebellum [31–33]. The sections without first antibody incubation were used as background control. According to the labeling intensity, the staining results were evaluated by two independent researchers and scored as negative (−) if no immunolabeling was observed in target cells, weakly positive (+) if the labeling was faint, and moderately to strongly positive (>++) when the labeling was stronger or distinctly stronger than (+). Before undertaking the above study, the experimental protocol was reviewed and approved by the ethnic committee of Dalian Medical University for protection of human subjects.

2.6. RNA Isolation and RT-PCR

Total cellular RNA was isolated from each of experimental group using Trizol solution (Life Technol., Grand Island, NY, USA). Reverse transcription (RT) was performed on RNA samples, followed by polymerase chain reaction (PCR) amplification. For RT, 0.5 μg of the RNA sample was added to 20 μL of RT reaction mixture (Takara, Inc., Ltd., Dalian, China) containing 4 μL of $MgCl_2$, 2 μL of 10× RNA PCR buffer, 9.5 μL of RNase-free distilled H_2O, 2 μL of dNTP mixture, 0.5 μL of RNase inhibitor, 1 μL of AMV reverse transcriptase, and 1 μL of oligo dT-adaptor primer. The reaction was carried out by treating the samples at 55 °C for 30 min, at 99 °C for 5 min, and at 5 °C for 5 min. PCR was conducted using the primers specific for each of the target genes (Table 1). Briefly, 2.5 μL of RT products were mixed with 16 μL of PCR-grade water, then with 6.5 μL of PCR working solution containing 1× PCR buffer, 1 μL of dNTP, 2.5 units of Taq DNA polymerase, and 50 pM upstream and downstream primers for SULT 1A1, SULT 1C2 and SULT 4A1, respectively. The PCR for individual genes were performed as follows: After initial denaturation for 5 min at 95 °C, samples were subjected to 35 cycles of 95 °C for 25 s; annealing temperature was 58 °C or 60 °C for 20 s and 72 °C for 20 s, with a final extension time of 2 min at 72 °C, and at 5 °C for 5 min. The PCR products were resolved on 1% agarose gel containing ethidium bromide (0.5 μg/mL). The bands were visualized and photographed using UVP Biospectrum Imaging System (UVP, Inc, Upland, CA, USA). The PCR products generated from the same RT solution by a pair of β-actin primers were cited as internal quantitative controls.

2.7. Protein preparation and Western blot analyses

Total cellular proteins were prepared from UW228-3 cells under different culture conditions by the method described previously [16]. Because of the impossibility to obtain normal brain tissues of humans, the corresponding tissues of rats were used as positive controls for SULTs. For Western blot analyses, the sample proteins (50 μg/lane) were separated by electrophoresis in 10% SDS-PAGE, transferred to polyvinylidene difluoride membrane (Amersham Biosci, Buckinghamshire, UK). The membrane was blocked with 5% skimmed milk in TBS-T (10 mM Tris–Cl, pH 8.0,

150 mM NaCl, and 0.5% Tween 20) at 4 °C overnight, rinsed three times (10 min each time) with TBS-T, followed by 2 h incubation at 37 °C with the first antibodies in appropriate concentrations (SULT1A1, 1:1200; SULT1C2, 1:500; SULT4A1, 1:600; β-actin, 1:3000) followed by 1 h incubation with HRP-conjugated anti-rabbit IgG (Zymed Lab Inc., San Francisco, CA, USA) at 37 °C. The bound antibody was detected using the enhanced chemiluminescence system (Roche Diagnostics GmbH, Mannheim, Germany). After removing the labeling signal by incubation with stripping buffer (62.5 mM Tris–HCl, pH 6.7, 100 mM 2-mercaptoethanol, 2% SDS) at 55 °C for 30 min, the membrane was reprobed with other antibodies one by one by the same experimental procedures until all of the parameters were examined.

2.8. Preparation of SULT-containing brain lysate

One female specific pathogen free Wistar rat was cultured in wire cages in a room maintained at 22 °C with a 12-h light/dark period at the Experimental Animal Center of Dalian Medical University. It was sacrificed by an animal expert in accordance with approved Ministerial procedures appropriate to the species. The brain tissue was rapidly obtained, snap frozen in liquid nitrogen and sectioned in 4 μm thickness at −40 °C; altogether 50 pieces of frozen slices were collected and homogenised in ice-cold buffer containing 250 mM sucrose, 1 mM DTT, 1× Mops buffer, which including 8 mM sodium acetate, 1 mM EDTA and 20 mM Mops (pH 7.0; Sigma Chem Co., St. Louis, MO, USA) [34]. The homogenates were subjected to differential centrifugation at 10,000 × *g* for 20 min at 4 °C, followed by 100,000 × *g* for 60 min at 1 °C using CP100MX ultracentrifuge (Hitachi Koki Co. Ltd., Tokyo, Japan). The resulting supernatant containing cytosolic sulfotransferase was kept at −80 °C and used within 24 h.

2.9. Resveratrol biotransformation and cell treatment

For sulfonating *trans*-resveratrol, a mixture (200 μL) containing 100 μL cytosolic proteins isolated from rat brain, 5 mM resveratrol, 2 mM PAPS (Sigma Chem Co., St. Louis, MO, USA), 1 mM DTT and 20 mM Mops buffer was prepared and incubated at 37 °C for 2 h. The reaction was terminated by standing the mixture-containing thin-wall tube on the boiling water for 5 min. The suspension was centrifuged at 10,000 × *g* for 5 min. 10 μL of the supernatant was subjected to HPLC and LC/MS analysis for fractionating resveratrol and its biotransformed metabolite(s), and the aliquots of the remaining part were used to treat UW228-3 cells in the total concentration of 100 μM. The cellular response(s) were checked with the parameters mentioned above. The cells treated by the chemical solution for brain lysate preparation, the brain lysate alone and the combination of resveratrol and brain lysate (without PAPS supplementation) were respectively used as background controls.

2.10. Statistical analyses

The experimental data were expressed as mean ± S.D. Mann–Whitney tests were used to analyze the statuses of SULT1A1, 1C2 and 4A1 expression in different histological groups and expressed in *p*-values. It was considered statistically significant if the *p*-value is less than 0.05.

3. Results

3.1. Resveratrol-sensitive features of UW228-3 cells

As shown in Fig. 1A, UW228-3 cells were elliptical without synaptophysin expression under normal culture condition; after being treated by 100 μM resveratrol for 48 h, the cells exhibited elongated fibrous phenotype with synaptophysin expression and showed distinct signs of apoptosis. Flow cytometry analyses (Fig. 1B) demonstrated that the G1 and S fractions were 48.50% and 45.97% in normally cultured UW228-3 cells, and changed to 97.62% and 1.26% in the cells treated by 100 μM resveratrol for 48 h. The percentages of apoptosis in UW228-3 cells were 3.67% before and 31.56% after 48-h resveratrol treatment. Accordingly, the 0.25% Trypan Blue evaluation revealed that after 100 μM resveratrol treatment for 0, 12, 24, 36, and 48 h, the percentages of unviable cells were 0.01%, 11.2%, 30.89%, 35.36%, and 42.86% respectively in the UW228-3 (Fig. 1C).

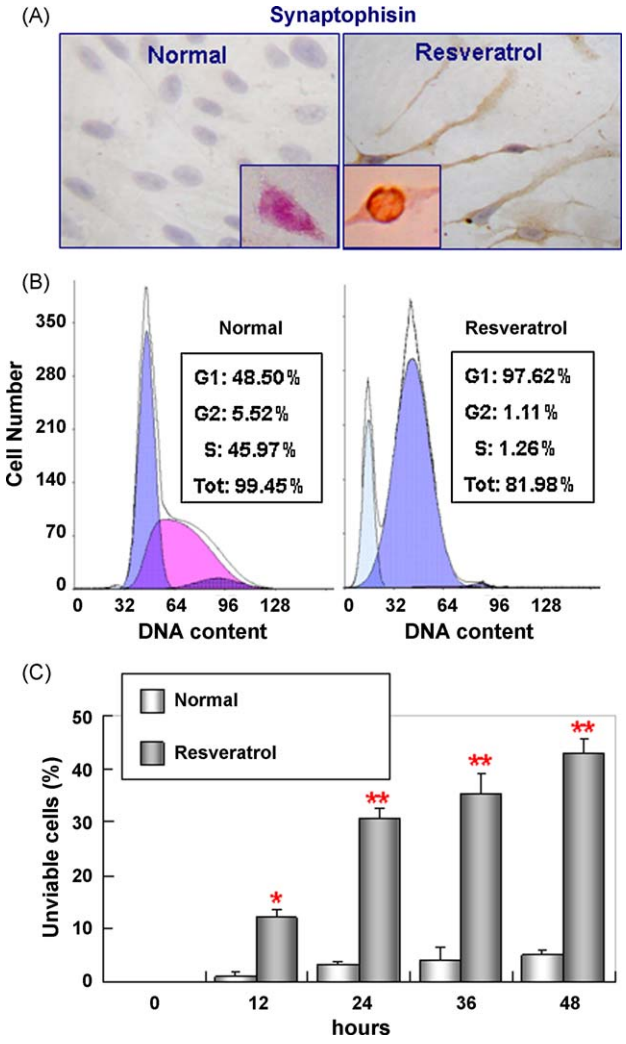

Fig. 1. Evaluation of chemosensitivities of UW228-3 cells to resveratrol. (A) To evaluate the chemosensitivity of UW228-3 cells, the cells were collected after incubation without (normal) or with 100 μM resveratrol for 48 h, and subjected to synaptophysin-oriented immunocytochemical staining and TUNEL apoptosis assay (shown in the small blocks of Fig. 1A). (B) After being cultured for 48 h, the cells without (normal) or with 100 μM resveratrol treatment were analyzed by flow cytometry. (C) Cells number was determined by Trypan Blue exclusion after 100 μM resveratrol incubation for 0, 12, 24, 36 and 48 h, respectively. Data are expressed as means ± S.D. ($n = 3$; $^{*}p < 0.01$; $^{**}p < 0.001$ vs. normal).

3.2. Metabolic pattern of resveratrol in UW228-3 cells

For identifying the resveratrol metabolites, UW228-3 cells were incubated with 100 μM resveratrol for 48 h. The cell pellets and the culture media were collected separately, cleaned up by SPE to eliminate the interferer and subjected to HPLC and LC–MS/MS analyses. Resveratrol-containing cell-free medium was used as

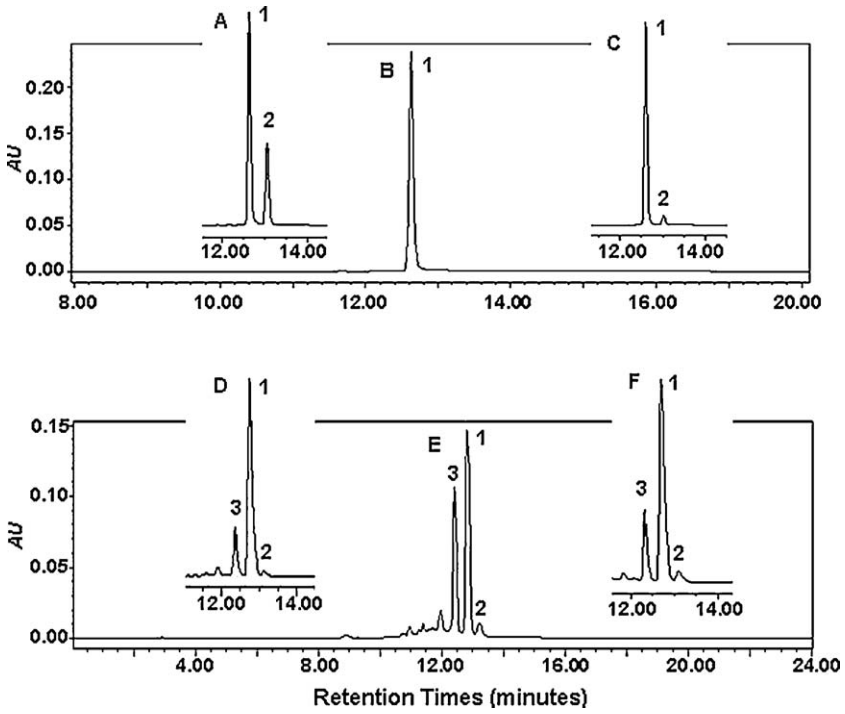

Fig. 2. HPLC-UV chromatography analysis. (A) *cis*-Resveratrol was prepared by exposure of *trans*-resveratrol-containing solution to natural light for 48 h, and analyzed by HPLC (t_{R1} = 12.63, t_{R2} = 13.09). (B) *trans*-Resveratrol standard was dissolved in methanol and analyzed by HPLC (t_{R1} = 12.61). (C) The culture media incubation with resveratrol without cells for 48 h, then was collected and analyzed by HPLC (t_{R1} = 12.62, t_{R2} = 13.01). (D) After UW228-3 cells treated with 100 μM resveratrol for 48 h, the cells lysate was analyzed by HPLC (t_{R1} = 12.67, t_{R2} = 13.12, t_{R3} = 12.38). (E) The supernatant of UW228-3 cells treated with 100 μM resveratrol for 48 h was analyzed by HPLC (t_{R1} = 12.71, t_{R2} = 13.19, t_{R3} = 12.38). (F) After UW228-3 cells treated with 100 μM resveratrol for 48 h, media containing resveratrol was removed and replaced with fresh media for another 24 h cultivation, then the supernatant was collected and analyzed by HPLC (t_{R1} = 12.69, t_{R2} = 13.09, t_{R3} = 12.31). t_R represents retention time of different compounds. (1) Represent *trans*-resveratrol; (2) represent *cis*-resveratrol; (3) represent resveratrol monosulfate.

background control. HPLC chromatogram analyses revealed that no less than 3 compounds could be detected in UW228-3 cells as well as the condition media (Fig. 2). In addition to resveratrol standard (*trans*-resveratrol), two additional major molecules were detected in the experimental samples (Fig. 2D–F). In contrast, only one extra molecule appeared in the resveratrol-containing cell-free medium stood in incubator for 24 h (Fig. 2C) and was later proved to be *cis*-resveratrol according to its retention time in HPLC and molecular weight in MS (Fig. 3).

3.3. Resveratrol monosulfate as major metabolite

According to the HPLC condition described above, the three major molecules were identified by LC–MS/MS using a combination of full and selected ion scanning techniques [35]. TIC of the condition media of UW228-3 cells treated with resveratrol for 48 h were listed in Fig. 3A. The peaks of M1, M2 and M3 could be detected from the chromatograms that represent *trans*-resveratrol (M1), *cis*-resveratrol (M2) and resveratrol monosulfate (M3), respectively. As illustrated in Fig. 3B, the negative ion mass spectrum of M1 (t_R = 13.61 min) showed a stable molecular ion at *m*/*z* 227. The CID spectrum of *m*/*z* 227 generated a series of fragment ions at 185 and 143 (Fig. 3B). The fragment ion at *m*/*z* 185 was generated from *m*/*z* 227 after loss of 42 amu (C_2H_2O), and the *m*/*z* 185 further fragmented to *m*/*z* 143 after loss of 42 amu (C_2H_2O), which corresponded to resveratrol [35]. The mass spectrum of M2 (t_R = 13.86 min) was shown in Fig. 3C. Although the retention time was longer for its polarity than the *trans*-resveratrol, the spectrum was identical to M1, and the fragment ions showed *m*/*z* at 185 and 143 attributed to resveratrol (Fig. 3C). Therefore, M2 was considered as the isomer of M1 [35]. The $[M-H]^-$ ion of M3 (t_R = 12.92 min) showed the deprotonated molecule ions of *m*/*z* 307 and 227, respectively, and the ion corresponding to resveratrol (*m*/*z* 227) through the neutral loss of the sulfate unit (*m*/*z* 80) from the resveratrol monosulfate, then the *m*/*z* 227 was fragmented to *m*/*z* 185 for the further loss of 42 amu (C_2H_2O) from resveratrol (Fig. 3D), which is proven to be the main characteristic fragmentation pathway [35], and the structure of M3 was concluded to resveratrol monosulfate as reported by other investigators [36].

The identities of the compounds were further confirmed by HRMS that gave the $[M-H]^-$ molecular ion exact mass as 227.0698 ($C_{14}H_{11}O_3$, calculated *m*/*z* 227.0708), 227.0697 ($C_{14}H_{11}O_3$, calculated *m*/*z* 227.0708), and 307.0261 ($C_{14}H_{11}SO_6$, calculated *m*/*z* 307.0276), which corresponded to *trans*-resveratrol, *cis*-resveratrol and resveratrol monosulfate, respectively (Table 3). Additionally, the resveratrol monosulfate could be detected in the condition media as early as 10 min of drug treatment, and its intracellular amount increased to the platform level at 12-h time point (Fig. 4), suggesting that the metabolic machinery pre-existed in the tumor cells and its efficiency was enhanced in response to resveratrol treatment. It was also noticed that the amounts of *trans*-resveratrol elevated at 24- and 48-h time points presumably due to the hydrolytic reaction that reversed resveratrol monosulfate to *trans*-resveratrol as proposed by Walle et al. [20,37]. Several additional small peaks were observed from the HPLC spectrum, but their chemical features were not further analyzed here because of their low amounts.

3.4. SULT expression before and after resveratrol treatment

It had been reported that SULT1A1, 1C2 and 4A1 were preferably expressed in human and rodent brains [32,38,39]. To investigate the responsibility of these three SULTs for resveratrol sulfation, the statuses of their expression in UW228-3 cells before and after resveratrol treatment were examined by RT-PCR,

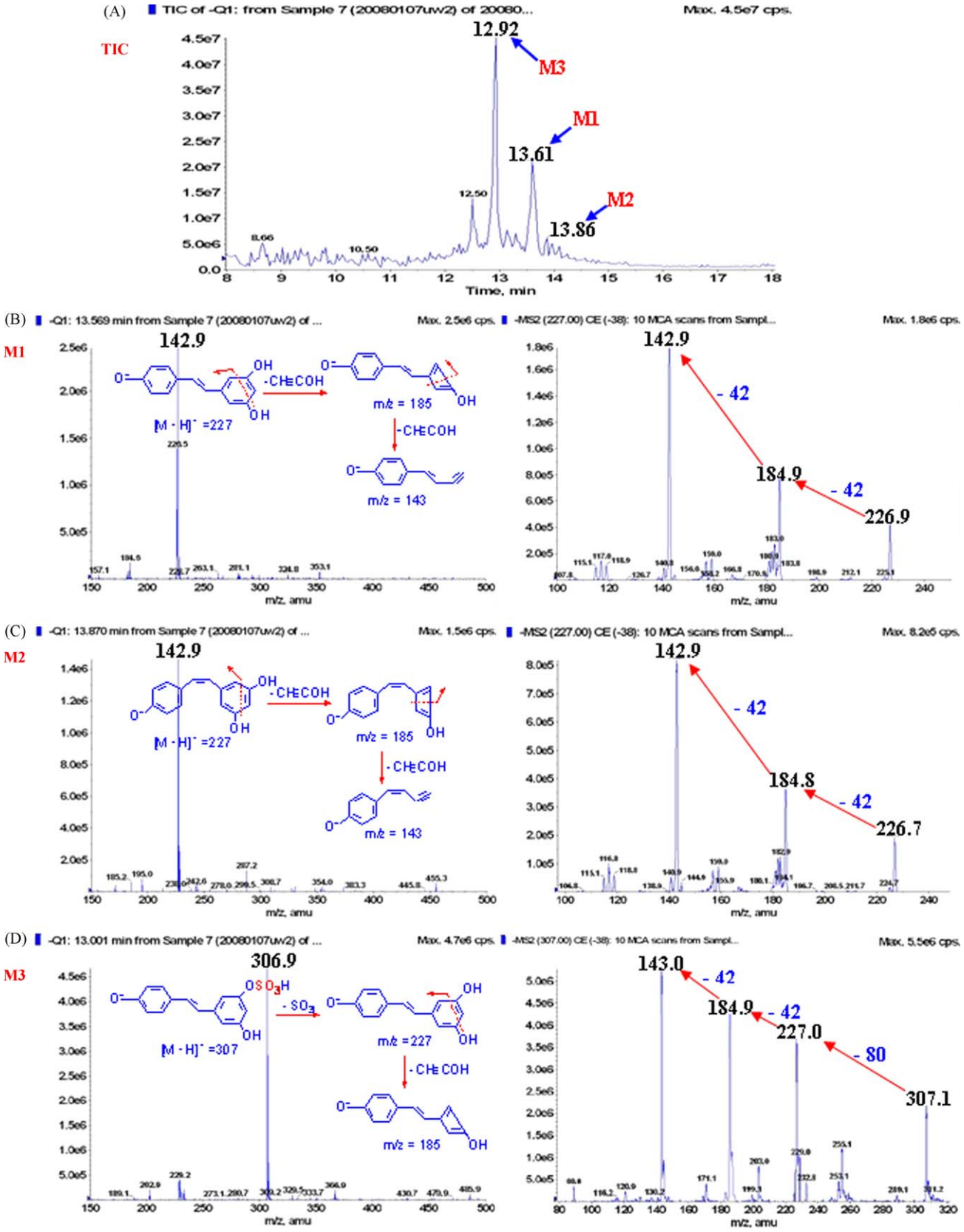

Fig. 3. MS analyses of resveratrol metabolites in UW228-3 cells. (A) Total ion chromatogram (TIC) of the supernatant of UW228-3 cells treated with 100 μM resveratrol for 48 h. Arrows labeled as M1, M2 and M3 indicate retention times corresponding to different mass composition of metabolites. (B), (C) and (D) indicate the MS1 and MS2 analysis of the different chromatographic peak M1, M2 and M3, which corresponding to different retention time. M1 represents *trans*-resveratrol; M2 represents *cis*-resveratrol; M3 represents resveratrol monosulfate.

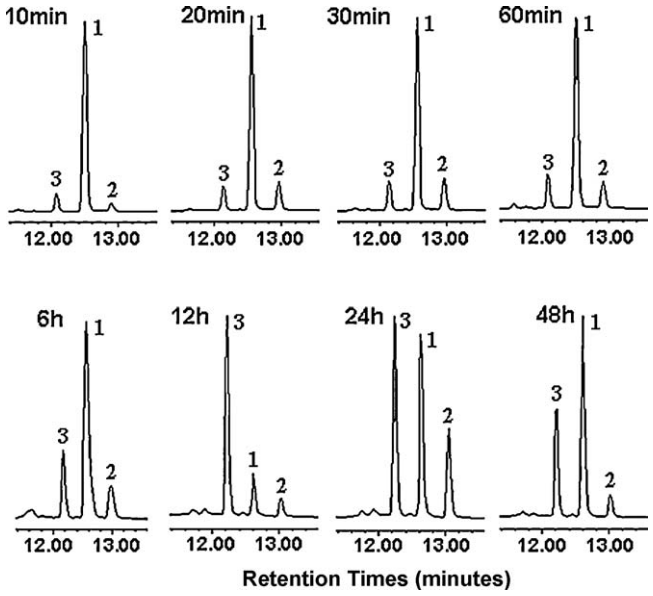

Fig. 4. Resveratrol metabolites in UW228-3 cells at different time points. The supernatant of UW228-3 cells were collected and purified by SPE respectively for HPLC analysis after 100 μM resveratrol treatment for (A) 10 min; (B) 20 min; (C) 30 min; (D) 60 min; (E) 6 h; (F) 12 h; (G) 24 h; (H) 48 h. Resveratrol monosulfate could be detected as early as 10 min of drug treatment, and its intracellular amount reached to the highest level at 12-h time point.

immunohistochemical staining and Western blotting. As shown in Fig. 5, the three brain-associated SULTs were constitutively expressed in normal rat cerebella and cerebrum. In UW228-3 cells, SULT1A1 was expressed in relatively normal level, whereas SULT 1C2 was expressed in low and SULT4A1 in extremely low levels. After resveratrol treatment, the level of SULT1A1 remained almost unchanged, while both SULT4A1 and 1C2 were enhanced, although their levels were still lower than that in the normal cerebella.

3.5. SULT down-regulation in medulloblastoma tissues

To elucidate whether the in vitro findings were hold true in vivo, IHC staining was performed on the tissue microarray constructed with human medulloblastomas and control samples. It was found that the overall expression levels of SULT1A1, 1C2 and 4A1 in the tumors were lower than that in tumor-surrounding noncancerous tissues and the rat normal brain (cerebella and cerebra) that were referred as normal controls for SULTs due to the impossibility to obtain fresh normal human brain tissues ([32]; Fig. 5B and Table 2). The results revealed that SULT1A1, 1C2 and 4A1 were absent in 24.3%, 10.8% and 8.1% and down-regulated in 43.2%, 64.9% and 29.7% of medulloblastoma cases, respectively. It was also noticed that the down-regulation patterns of the three SULTs were not identical in different cases irrespective to the similarity of their morphology (Fig. 5B).

3.6. Reduced effects of cis-resveratrol and resveratrol monosulfate

cis-Resveratrol was prepared by standing 100 μM *trans*-resveratrol under natural light for 48 h [26]. After confirming 50% transition of *cis*-resveratrol in the stock solution by HPLC and LC/MS analysis (Fig. 6B and Table 3), this *trans*- and *cis*-resveratrol mixture was used to treat UW228-3 cells for 48 h in a final concentration of 100 μM. Unlike the original reagent, the *cis*-resveratrol-enriched solution exhibited little influence on anti-medulloblastoma activity in terms of growth inhibition, neuron-like differentiation and apoptosis induction (Fig. 6C and D). On the other hand, *trans*-resveratrol was incubated in the brain lysates for 2 h and then analyzed by HPLC and LC/MS. It was also revealed that the monosulfate was the major metabolite and about 1/2 of parent *trans*-resveratrol was biotransformed to resveratrol monosulfate (Fig. 6B). In difference with the situation of 100 μM *trans*-resveratrol treatment, UW228-3 cells treated by the same concentration of this mixture for 48 h showed neither distinct growth suppression nor the signs of neuron-oriented differentiation and apoptosis (Fig. 6C and D). As shown in Fig. 6C, PAPS-containing brain lysate alone (B) exerted little effected on cell growth and the anti-medulloblastoma efficacy of resveratrol was not influenced by brain lysate without PAPS supplementation (B + R). Similarly, no observable cellular change could be found in the cells treated by 10 μL of the chemical solution for brain lysate preparation (data not shown).

4. Discussion

An ideal cancer therapeutic agent should have minimal cytotoxicity to normal tissues, meanwhile, exerts crucial effects on cancer cells. Resveratrol is such candidate, because of its nontoxic property and anticancer activities in a variety of human and rodent cancers [40]. It has been recognized that resveratrol undergoes intracellular enzymatic biotransformation that generates one or more metabolites [36,41]. However, the pharmaceutical potentials of those metabolic products have not yet been well ascertained. Some researchers proposed that resveratrol metabolite(s) such as resveratrol sulfates or resveratrol glucuronides were the bioactive forms because of the low bioavailability of parent *trans*-resveratrol in vivo [37], while others considered that *trans*-resveratrol by itself was sufficient to cause vital cellular and molecular consequences in the treated cancer cells [40,42,43]. Apparently, determination of the bioactive form(s) of resveratrol in individual cell and cancer types becomes a fundamental issue for the successful application of resveratrol in preventive and clinical medicine. In this context, a comparison of resveratrol metabolic pattern in resveratrol-sensitive cancer cells would be helpful in figuring out this point. According to our previous observation, several medulloblastoma cell lines including UW228-3 were sensitive to resveratrol in terms of growth arrest, neuronal-oriented differentiation and apoptosis [11]. Therefore, those cells may serve as an ideal experimental model to identify the anticancer form(s) of resveratrol.

The main approach for identification of drug metabolites is the combined use of HPLC, MS and LC–MS/MS techniques, which is based on the different retention time, the polarity and m/z ratio of the molecules [44,45]. We therefore adopted them for profiling the resveratrol metabolites in resveratrol-sensitive UW228-3 cells. As the first finding, we detected *cis*-resveratrol in the condition media of UW228-3 cells. Further analysis revealed that *cis*-resveratrol could also be generated by standing the cell-free resveratrol-containing medium in incubator for 48 h. These phenomena indicated that *cis*-resveratrol was not a metabolic product but a spontaneously formed isomer of *trans*-resveratrol during the experiment [46]. Unlike *trans*-resveratrol, the data about the anticancer aspect of *cis*-resveratrol were quite limited. To address potential effect of *cis*-resveratrol on medulloblastoma cells, a mixture-containing high fraction (about 50%) of *cis*-resveratrol was prepared by exposing 100 μM *trans*-resveratrol medium under natural light at room temperature for 48 h [26], and then used to treat UW228-3 cells. The results revealed an obvious reduction of anti-medulloblastoma efficacy of this mixture in terms of less differentiation and apoptosis tendencies of UW228-3 cells. This result thus suggests, at least for medulloblastoma cells, that *trans*-resveratrol rather than its *cis*-counterpart possesses powerful anticancer capacity. In consideration of the unstable

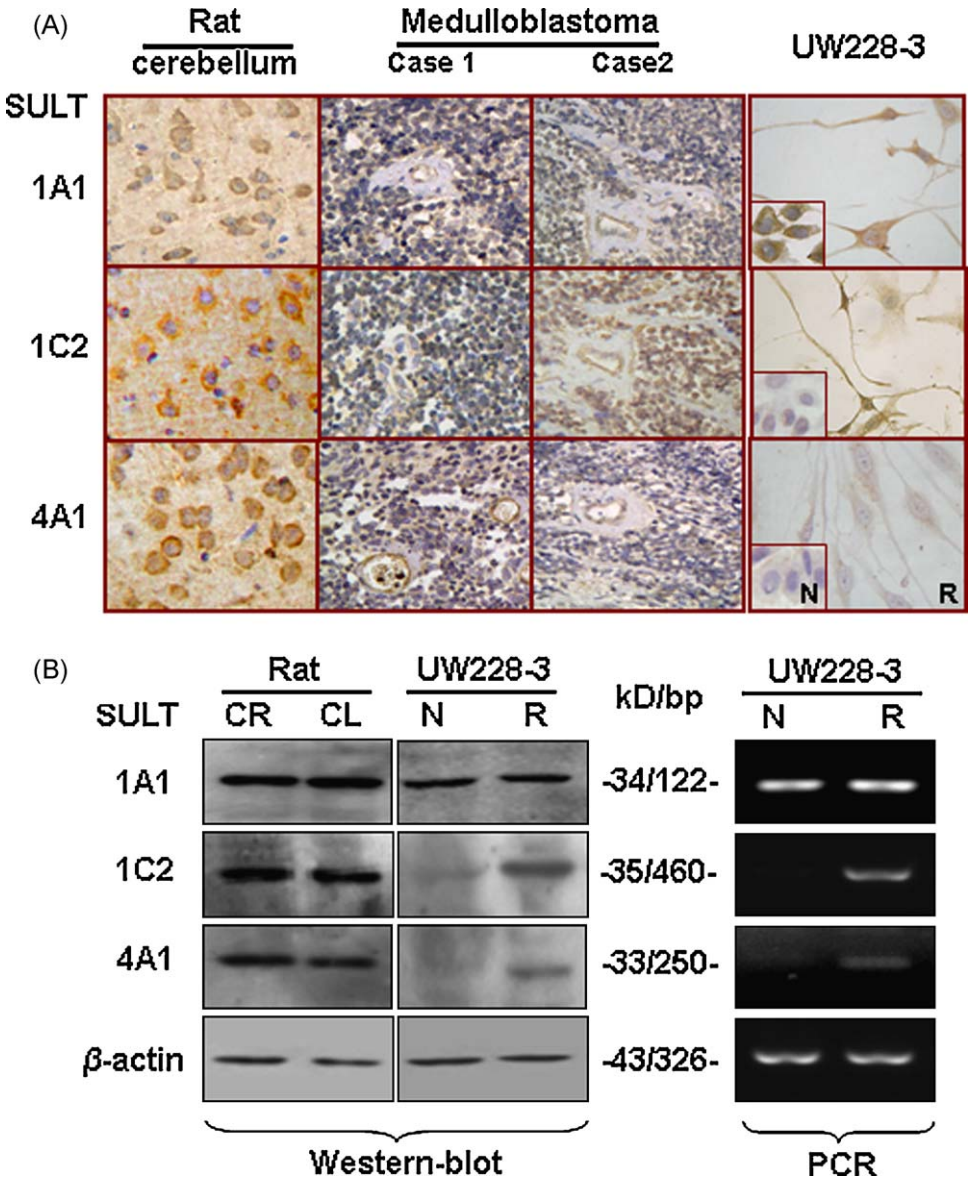

Fig. 5. Evaluation of SULT1A1, 1C2 and 4A1 expression. (A) Immunohistochemical illustration of differential patterns of three brain-associated SULT expression in normal rat cerebellum, two medulloblastoma cases and UW228-3 cells without (N) and with (R) resveratrol treatment. (B) Western blot and PCR analyses of SULT1A1, 1C2 and 4A1 expression in normal rat cerebrum (CR), cerebellum (CL) and UW228-3 cells without (N) and with (R) 100 μM resveratrol treatment. β-Actin was used as loading control.

chemical feature of this reagent, *trans*-resveratrol should be prepared freshly and handled with care to maintain its chemotherapeutic activity during experiments and clinical practice.

The drug metabolic reactions can be classified into phase I and phase II reactions. Phase I reactions usually precede phase II and introduce the functional groups such as the hydroxyl group to the metabolites. In phase II reactions such as sulfation, the polar functional groups of phase I metabolites are conjugated with an endogenous molecule, leading to the increased solubility of the xenobiotics for an active extracellular excretion and drug activation or inactivation [47]. Resveratrol monosulfate identified in the lysate and condition media of UW228-3 cells is the phase II metabolic product. Since sulfation reaction is mediated by SULTs, the levels of SULT expression may positively or negatively influence resveratrol

Table 2
Tissue microarray-based immunohistochemical profiling of brain-associated SULT expression in different brain tissues.

Samples	No.	SULT1A1 (%)			SULT1C2 (%)			SULT4A1 (%)		
		− $	+	>++	−	+	>++	−	+	>++
Rat cerebellum	19	0 (0)	0 (0)	19 (100)	0 (0)	7 (36.84)	12 (63.16)	0 (0)	0 (0)	19 (100)
Surgical specimens	47									
Noncancerous	10	0 (0)	0 (0)	10 (100)	0 (0)	9 (90.0)	1 (10.0) *	0 (0)	0 (0)	10 (100)
Tumor	37	9 (24.3)	16 (43.2)	12 (32.4)*,#	4 (10.8)	24 (64.9)	9 (24.3)*	4 (10.8)	13 (35.1)	20 (54.1)*,#

(* or #) represents statistical significance ($p < 0.01$) respectively.
(*) Compared with rat cerebellum; (#) compared with noncancerous.
($ −) Negative in immuno-labeling was observed in target cells; (+) weakly positive in immuno-labeling; (++) stronger immuno-labeling.

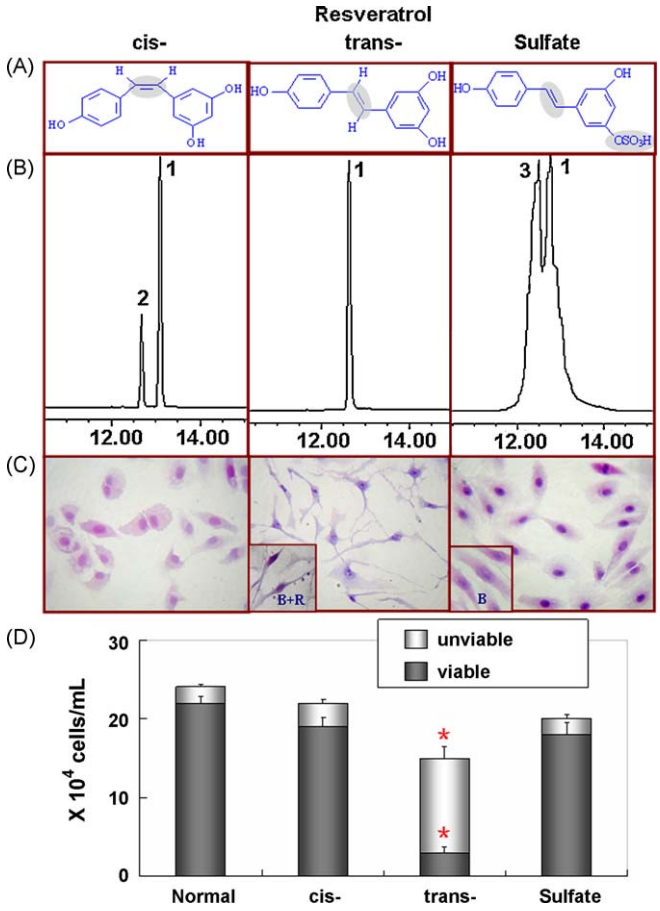

Fig. 6. Biotransformation and distinct biological effects of *trans*-resveratrol, *cis*-resveratrol and resveratrol monosulfate on UW228-3 cells. (A) The chemical structures of *trans*-resveratrol, *cis*-resveratrol and resveratrol monosulfate; (B) HPLC analysis of the efficiencies of resveratrol biotransformation. (1), (2) and (3) represent *trans*-resveratrol, *cis*-resveratrol and resveratrol monosulfate, respectively. (C) Morphologic evaluation of UW228-3 cells incubated with 100 μM of *trans*-resveratrol (*trans*-), *trans*-resveratrol/*cis*-resveratrol mixture (*cis*-), and *trans*-resveratrol/resveratrol monosulfate mixture (sulfate) for 48 h by H&E staining (40×). The cells treated by PAPS-containing brain lysate (B) and by 100 μM resveratrol and PAPS-absent brain lysate combination were cited as background controls (the images in the small blocks in Fig. 6C). (D) Trypan Blue discrimination of stained (unviable) and unstained (viable) cells. The column indicates the number of viable cells; (*) $p < 0.001$.

bioactivity. Of the members of SULT super-family, SULT1A1, 4A1 and 1C2 are preferably expressed in the rodent brain [31–33]. For these reasons, we checked the statuses of those three brain-associated SULT enzymes in UW228-3 cells, medulloblastoma tissues, tumor-surrounding cerebella and the normal rat brain (cerebella and cerebra). In comparison with the noncancerous tumor-surrounding cerebella and normal rat brain tissues, the expression levels of the three SULTs were low in UW228-3 cells before and after resveratrol treatment. In agreement of in vitro findings, overall down-regulation of SULT1A1, 1C2 and 4A1 expression was found in the medulloblastomas so far checked. These data suggest that the sulfation activity in medulloblastoma cells were lower than that in the normal brain and the tumor-surrounding cerebella. Given the resveratrol-sensitive feature of UW228-3 cells, it might be possible that SULT-mediated sulfation reduces resveratrol bioavailability via modifying the chemical structure, facilitating the drug excretion and, consequently, shortening the retention time of *trans*-resveratrol in the host cells. From this point of view, the reduction of SULT expression may be a favorable factor for achieving better therapeutic outcome through maintaining an effective dose of *trans*-resveratrol in cancer cells. To prove this speculation, it is necessary to identify the bioactive form(s) of resveratrol by treating UW228-3 cells with resveratrol monosulfate and to see what cellular and molecular events would happen to the cells.

Table 3
MS1 and MS2 analysis of resveratrol biotransformation.

MS1 ions (m/z) $[M-H]^-$	MS2 product ions		Identification
	m/z	Fragment loss	
227	185	$[M-H-42]^-$	Standard resveratrol
	143	$[M-H-84]^-$	
227	185	$[M-H-42]^-$	*trans*-Resveratrol
	143	$[M-H-84]^-$	
227	185	$[M-H-42]^-$	*cis*-Resveratrol
	143	$[M-H-84]^-$	
307	227	$[M-H-80]^-$	Resveratrol monosulfate
	185	$[M-H-80-42]^-$	
	143	$[M-H-80-84]^-$	

Identification of bioactive form of resveratrol is an important issue for successful application of this reagent in clinic. However, the data about the pharmaceutical activities of *trans*-resveratrol and its conjugates are controversial [20]. To clarify this point, we prepared the resveratrol monosulfate by treating *trans*-resveratrol with rat brain lysate that was rich in sulfotransferases, especially SULT1A1, 1C2 and 4A1 [32,38]. After ascertaining the efficiency of biotransformation (about 50%) by LC/MS analyses, the resultant mixture was used to treat UW228-3 cells. In comparison with the outcome of the conventional 100 μM resveratrol treatment, the pre-incubation with brain lysate apparently reduced anti-medulloblastoma effect of *trans*-resveratrol because of the lack of differentiation and apoptosis phenomena in the treated cells. Since 10 μL brain lysate and the chemical solution from which the brain lysate was prepared did not give rise to observable alteration of UW228-3 cells, their possible cytotoxic effects on the treated cells can be largely ruled out. Consequently, our current results indicate that resveratrol monosulfate has less pharmaceutical impact on UW228-3 cells, although the approach of in vitro resveratrol biotransformation needs to be further improved. From this point of view, the constitutive and up-regulatable expression of SULTs in normal rat brain may dynamically balance the bioavailability of *trans*-resveratrol to the amounts that are tolerable for healthy organs and individuals. On the other hand, the overall low SULT expression level and the less sensitivity of SULT genes to resveratrol in UW228-3 cells may prolong the interactions of *trans*-resveratrol and its molecular targets and create vital biological events. As an alternative approach to further testify this speculation, it would be worthwhile to transfect SULT-expressing element to UW228-3 cells and to elucidate SULT expression pattern in resveratrol-resistant brain tumors.

Taken together, this study revealed that *trans*-resveratrol was chemically unstable and its anti-medulloblastoma activity was attenuated by spontaneously generated *cis*-resveratrol. Resveratrol monosulfate was the major metabolite of medulloblastoma cells and its generation may reduce the anti-medulloblastoma efficacy of *trans*-resveratrol. In comparison with the expression levels in the tumor-surrounding tissues and rat normal brains, the three brain-associated SULT genes were absent or down-regulated in medulloblastoma cells in vivo and in vitro and this situation kept almost unchanged in resveratrol-treated UW228-3 cells, indicating the overall low sulfation activity in medulloblastoma cells. It is therefore demonstrated that the efficiency of metabolic reduction of *trans*-resveratrol is the major determinant of the fate of resveratrol-treated medulloblastoma cells. These findings would be of translational values in exploring tumor-selective and personalized application of resveratrol in cancer prevention and treatment.

Acknowledgments

We gratefully acknowledge Hui Wang, Jing-Ping Cao and Ying Gao for their assistance with the HPLC and LC/MS detection. We thank Drs. Xin-Feng Zhao and Peng Gao for their assistance with the HRMS analysis and Professor Xiang-Hong Yang for providing human medulloblastoma specimens. This work is supported by the grants from National Natural Science Foundation of China (Nos. 30527002, 30670946 and 30971038) and by the special grants of Liaoning Department of Education for the key laboratory (20060193) and for the creative research team (2007-7-26 and 2008T028).

References

[1] Jang M, Cai L, Udeani GO, Slowing KV, Thomas CF, Beecher CW, et al. Cancer chemopreventive activity of resveratrol, a natural product derived from grapes. Science 1997;275:218–20.
[2] Dixon RA. Natural products and plant disease resistance. Nature 2001;411:843–7.
[3] Rivera L, Morón R, Zarzuelo A, Galisteo M. Long-term resveratrol administration reduces metabolic disturbances and lowers blood pressure in obese Zucker rats. Biochem Pharmacol 2009;77:1053–63.
[4] Burstein B, Maguy A, Clément R, Gosselin H, Poulin F, Ethier N, et al. Effects of resveratrol (*trans*-3,5,4′-trihydroxystilbene) treatment on cardiac remodeling following myocardial infarction. J Pharmacol Exp Ther 2007;323:916–23.
[5] Olas B, Wachowicz B. Resveratrol and vitamin C as antioxidants in blood platelets. Thromb Res 2002;106:143–8.
[6] Zhu J, Yong W, Wu X, Yu Y, Lv J, Liu C, et al. Anti-inflammatory effect of resveratrol on TNF-alpha-induced MCP-1 expression in adipocytes. Biochem Biophys Res Commun 2008;369:471–7.
[7] Shakibaei M, Csaki C, Nebrich S, Mobasheri A. Resveratrol suppresses interleukin-1beta-induced inflammatory signaling and apoptosis in human articular chondrocytes: potential for use as a novel nutraceutical for the treatment of osteoarthritis. Biochem Pharmacol 2008;76:1426–39.
[8] Hudson TS, Hartle DK, Hursting SD, Nunez NP, Wang TT, Young HA, et al. Inhibition of prostate cancer growth by muscadine grape skin extract and resveratrol through distinct mechanisms. Cancer Res 2007;67:8396–405.
[9] Aziz MH, Reagan-Shaw S, Wu J, Longley BJ, Ahmad N. Chemoprevention of skin cancer by grape constituent resveratrol: relevance to human disease? FASEB J 2005;19:1193–5.
[10] Boissy P, Andersen TL, Abdallah BM, Kassem M, Plesner T, Delaissé JM. Resveratrol inhibits myeloma cell growth, prevents osteoclast formation, and promotes osteoblast differentiation. Cancer Res 2005;65:9943–52.
[11] Zhang P, Li H, Wu ML, Chen XY, Kong QY, Wang XW, et al. c-Myc downregulation: a critical molecular event in resveratrol-induced cell cycle arrest and apoptosis of human medulloblastoma cells. J Neurooncol 2006;80:123–31.
[12] Danz ED, Skramsted J, Henry N, Bennett JA, Keller RS. Resveratrol prevents doxorubicin cardiotoxicity through mitochondrial stabilization and the Sirt1 pathway. Free Radic Biol Med 2009;46:1589–97.
[13] Venkatesan B, Ghosh-Choudhury N, Das F, Mahimainathan L, Kamat A, Kasinath BS, et al. Resveratrol inhibits PDGF receptor mitogenic signaling in mesangial cells: role of PTP1B. FASEB J 2008;22:3469–82.
[14] Wang Q, Xu J, Rottinghaus GE, Simonyi A, Lubahn D, Sun GY, et al. Resveratrol protects against global cerebral ischemic injury in gerbils. Brain Res 2002;958:439–47.
[15] Wang Q, Li H, Liu N, Chen XY, Wu ML, Zhang KL, et al. Correlative analyses of notch signaling with resveratrol-induced differentiation and apoptosis of human medulloblastoma cells. Neurosci Lett 2008;438:168–73.
[16] Yu LJ, Wu ML, Li H, Chen XY, Wang Q, Sun Y, et al. Inhibition of STAT3 expression and signaling in resveratrol-differentiated medulloblastoma cells. Neoplasia 2008;10:736–44.
[17] Bishayee A. Cancer prevention and treatment with resveratrol: from rodent studies to clinical trials. Cancer Prev Res 2009;2:409–18.
[18] Li Y, Bäckesjö CM, Haldosén LA, Lindgren U. Resveratrol inhibits proliferation and promotes apoptosis of osteosarcoma cells. Eur J Pharmacol 2009;609:13–8.
[19] Woo KJ, Lee TJ, Lee SH, Lee JM, Seo JH, Jeong YJ, et al. Elevated gadd153/chop expression during resveratrol-induced apoptosis in human colon cancer cells. Biochem Pharmacol 2007;73:68–76.
[20] Gescher AJ, Steward WP. Relationship between mechanisms, bioavailibility, and preclinical chemopreventive efficacy of resveratrol: a conundrum. Cancer Epidemiol Biomarkers Prev 2003;12:953–7.
[21] Ellison DW, Onilude OE, Lindsey JC, Lusher ME, Weston CL, Taylor RE, et al. Beta-catenin status predicts a favorable outcome in childhood medulloblastoma: the United Kingdom Children's Cancer Study Group Brain Tumour Committee. J Clin Oncol 2005;23:7951–7.
[22] Marino S. Medulloblastoma: developmental mechanisms out of control. Trends Mol Med 2005;11:17–22.
[23] Liu J, Guo L, Luo Y, Li JW, Li H. All *trans*-retinoic acid suppresses in vitro growth and down-regulates LIF gene expression as well as telomerase activity of human medulloblastoma cells. Anticancer Res 2000;20:2659–64.
[24] Wang Q, Li H, Wang XW, Wu DC, Chen XY, Liu J. Resveratrol promotes differentiation and induces Fas-independent apoptosis of human medulloblastoma cells. Neurosci Lett 2003;351:83–6.
[25] Keles GE, Berger MS, Srinivasan J, Kolstoe DD, Bobola MS, Silber JR. Establishment and characterization of four human medulloblastoma-derived cell lines. Oncol Res 1995;7:493–503.
[26] Chen X, He H, Wang G, Yang B, Ren W, Ma L, et al. Stereospecific determination of *cis*- and *trans*-resveratrol in rat plasma by HPLC: application to pharmacokinetic studies. Biomed Chromatogr 2007;21:257–65.
[27] Mercolini L, Addolorata Saracino M, Bugamelli F, Ferranti A, Malaguti M, Hrelia S, et al. HPLC-F analysis of melatonin and resveratrol isomers in wine using an SPE procedure. J Sep Sci 2008;31:1007–14.
[28] Qian G, Leung SY, Lu G, Leung KS. Optimization and validation of a chromatographic method for the simultaneous quantification of six bioactive compounds in Rhizoma et Radix Polygoni Cuspidati. J Pharm Pharmacol 2008;60:107–13.
[29] Boocock DJ, Patel KR, Faust GE, Normolle DP, Marczylo TH, Crowell JA, et al. Quantitation of *trans*-resveratrol and detection of its metabolites in human plasma and urine by high performance liquid chromatography. J Chromatogr B 2007;848:182–7.
[30] Urpi-Sarda M, Zamora-Ros R, Lamuela-Raventos R, Cherubini A, Jauregui O, de la Torre R, et al. HPLC-tandem mass spectrometric method to characterize resveratrol metabolism in humans. Clin Chem 2007;53:292–9.
[31] Salman ED, Kadlubar SA, Falany CN. Expression and localization of cytosolic sulfotransferase (SULT) 1A1 and SULT1A3 in normal human brain. Drug Metab Dispos 2009;37:706–9.
[32] Liyou NE, Buller KM, Tresillian MJ, Elvin CM, Scott HL, Dodd PR, et al. Localization of a brain sulfotransferase, SULT4A1, in the human and rat brain: an immunohistochemical study. J Histochem Cytochem 2003;51:1655–64.
[33] Allali-Hassani A, Pan PW, Dombrovski L, Najmanovich R, Tempel W, Dong A, et al. Structural and chemical profiling of the human cytosolic sulfotransferases. PLoS Biol 2007;5:1063–78.
[34] Hui Y, Yasuda S, Liu MY, Wu YY, Liu MC. On the sulfation and methylation of catecholestrogens in human mammary epithelial cells and breast cancer cells. Biol Pharm Bull 2008;31:769–73.
[35] Wang DG, Hang TJ, Wu CY, Liu WY. Identification of the major metabolites of resveratrol in rat urine by HPLC-MS/MS. J Chromatogr B 2005;829:97–106.
[36] Murias M, Miksits M, Aust S, Spatzenegger M, Thalhammer T, Szekeres T, et al. Metabolism of resveratrol in breast cancer cell lines: impact of sulfotransferase 1A1 expression on cell growth inhibition. Cancer Lett 2008;261:172–81.
[37] Walle T, Hsieh F, DeLegge MH, Oatis JE, Walle UK. High absorption but very low bioavailability of oral resveratrol in humans. Drug Metab Dispos 2004;32:1377–82.
[38] Alnouti Y, Klaassen CD. Tissue distribution and ontogeny of sulfotransferase enzymes in mice. Toxicol Sci 2006;93:242–55.
[39] Lindsay J, Wang LL, Li Y, Zhou SF. Structure, function and polymorphism of human cytosolic sulfotransferases. Curr Drug Metab 2008;39:99–105.
[40] Baur JA, Sinclair DA. Therapeutic potential of resveratrol: the in vivo evidence. Nat Rev Drug Discov 2006;5:493–506.
[41] Lançon A, Hanet N, Jannin B, Delmas D, Heydel JM, Lizard G, et al. Resveratrol in human hepatoma HepG2 cells: metabolism and inducibility of detoxifying enzymes. Drug Metab Dispos 2007;35:699–703.
[42] Howitz KT, Bitterman KJ, Cohen HY, Lamming DW, Lavu S, Wood JG, et al. Small molecule activators of sirtuins extend *Saccharomyces cerevisiae* life span. Nature 2003;425:191–6.
[43] Lee SK, Zhang W, Sanderson BJ. Selective growth inhibition of human leukemia and human lymphoblastoid cells by resveratrol via cell cycle arrest and apoptosis induction. J Agric Food Chem 2008;56:7572–7.
[44] Holcapek M, Kolárová L, Nobilis M. High-performance liquid chromatography-tandem mass spectrometry in the identification and determination of phase I and phase II drug metabolites. Anal Bioanal Chem 2008;391:59–78.
[45] Yang J, Zhao XJ, Liu XL, Wang C, Gao P, Wang JS, et al. High performance liquid chromatography-mass spectrometry for metabonomics: potential biomarkers for acute deterioration of liver function in chronic hepatitis B. J Proteome Res 2006;5:554–61.
[46] Pervaiz S. Resveratrol: from grapevines to mammalian biology. FASEB J 2003;17:1975–85.
[47] Liska D, Lyon M, Jones DS. Detoxification and biotransformational imbalances. Explore (NY) 2006;2:122–40.